

The (π^+ , πN) Reactions on Carbon at 130 MeV: A Bubble-Chamber Experiment.

E. BELLOTTI, S. BONETTI, D. CAVALLI and C. MATTEUZZI

Istituto di Fisica dell'Università - Milano

Istituto Nazionale di Fisica Nucleare - Sezione di Milano

(ricevuto il 30 Ottobre 1972)

Summary. — The (π^+ , πN) reactions at ~ 130 MeV (kinetic energy) have been investigated by means of a propane bubble chamber. About 250 events of quasi-elastic scattering on bound protons of the p and s shells have been analysed and the results compared with the predictions of the impulse approximation model (IAM): the agreement is generally good. We obtained the following results: the best values for the parameter A appearing in the harmonic-oscillator form factors are $A_p = (160 \pm 10)$ MeV/c and $A_s = (300 \pm 30)$ MeV/c for p - and s -shell protons respectively; the total cross-section for the (π^+ , π^+p) reaction is (66 ± 10) mb and the ratio between the cross-sections for the separation of a p - or a s -proton is 1.5 ± 0.2 . About 100 charge exchange events have been collected; the corresponding cross-section is (36 ± 5) mb, while the estimated σ for (π^+ , π^0p) is (18 ± 3) mb. In the limit of the statistics it seems that also this reaction can be explained on the basis of the IAM. Data concerning the reactions (π^+ , π^+n) based on ~ 100 events show some discrepancies with the IAM predictions which cannot be easily explained by the poor statistics and by the difficulties of the experimental analysis. The ratio between the cross-sections for separation of a p and of a n is 1.7 ± 0.2 .

Introduction.

The study of the (π , πN) reactions in the region of the Δ -resonance is particularly attractive. The experimental result of CHIVERS *et al.* ⁽¹⁾ on the

⁽¹⁾ D. T. CHIVERS, E. M. RIMMER, B. W. ALLARDYCE, R. C. WITCOMB, S. S. DOMINGO and N. W. TANNER: *Nucl. Phys.*, **126 A**, 129 (1969).

ratio

$$R = \frac{\sigma_{(\pi^-, \pi^- n)}}{\sigma_{(\pi^+, \pi^+ n + \pi^0 p)}}$$

measured for even-even light nuclei is not justified by a simple impulse approximation calculation.

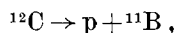
The aim of the present bubble chamber experiment ⁽²⁾ is the study of the reaction



induced by π^+ at ~ 130 MeV of kinetic energy. The use of a bubble chamber permits a complete kinematical reconstruction of the events. The analysis of reaction (1) allowed us:

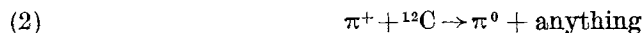
the check of the impulse approximation model (IAM) on differential cross-sections,

the estimation of the form factor for the virtual decay



the evaluation of the ratio σ_p/σ_s between the cross-section for the separation of a proton from the p and s shells.

In the same time some experimental information on the charge exchange reaction



and on the scattering on bound neutron



have been obtained. While a detailed analysis of (2) and (3) is not possible owing to the experimental limitations, our data are sufficient to check their compatibility with the IAM and to roughly estimate their cross-sections.

A short description of the experimental apparatus and of the criteria followed in selecting and measuring the events will be given in Sect. 1. A brief outline of the IAM formulae and of the distortions introduced by the experimen-

⁽²⁾ E. BELLOTTI, S. BONETTI, E. FIORINI, A. PULLIA and M. ROLLIER: *Preliminary results on interactions of low-energy pions on carbon nuclei*, in *High-Energy Physics and Nuclear Structure* (New York, 1970), p. 461; E. BELLOTTI, S. BONETTI, D. CAVALLI and E. FIORINI: *Proceedings of the Topical Seminar on Interactions of Elementary Particles with Nuclei* (Trieste, 1970), p. 369.

tal apparatus is reported in Sect. 2. Section 3 is devoted to the analysis and to the comparison of the data with the theoretical predictions; finally the results will be discussed and compared with other data in Sect. 4.

1. – Experimental details.

1.1. *Chamber and beam.* – The Ecole Polytechnique heavy-liquid bubble chamber ($(100 \times 50 \times 50)$ cm³), filled with pure propane (radiation length ~ 110 cm) was exposed in Saclay to π^+ separated beams at different momenta ranging from 300 to 2000 MeV/c. For the present investigation the pictures obtained at the lowest energy (~ 160 MeV) have been analysed. Due to the energy loss in the liquid, the kinetic energy of interacting π 's is somewhat lower than the beam energy. The characteristics of the exposure are:

Number of pictures	Magnetic field (kG)	T_{beam} (MeV)	T_{int} (MeV)	ΔT (MeV)
11 000	10.5	160	$115 \div 150$	≤ 7

1.2. *Selection of the events.* – The pictures have been scanned for all the interactions occurring in a suitable fiducial volume. The events

a) with a π^+ in the final state, regardless of the number of the associated protons,

b) with at least a (e^+ , e^-) pair of a fast Compton electron pointing towards a primary interaction

have been retained for the present analysis.

Events of type *a)*: Only those events where the emitted particles stop in the chamber have been accepted; the kinetic energy of a particle is calculated from its range and it is affected by a small error ($(1 \div 2)\%$). This requirement made it possible to select the events due to interaction on protons of the *p*- or *s*-shell from the sample of events having a π^+ and a *p* in the final state. This cut-off also eliminates a large fraction of elastic scattering on C in the sample of events having one π^+ and no *p*'s in the final state. The number of selected events, according to the multiplicity of visible protons ($l > 4$ mm) is

π^+-0 p	π^+-1 p	π^+-2 p
192 (72)	915 (37)	37

(the numbers in brackets refer to interaction accompanied by a short not measurable track, *i.e.* a blob).

Events of type *b)*: About 100 events marked by at least a γ -ray associated to the primary vertex, have been found. According to the proton multiplicity

they are

π^0 -0 p	π^0 -1 p	π^0 -2 p
18 (4)	69 (9)	12

1'3. π^+p final state. - Let us consider first the sample of events with one visible proton in the final state; it contains both interactions on C and on H; though the last ones must be eliminated, they are very useful to check the whole experimental procedure.

The missing energy

$$E_m = T_{\pi_{\text{inc}}} - T_{\pi_{\text{out}}} - T_p,$$

where T 's are the kinetic energy of the incoming and outgoing π 's and p, is calculated for each event; its distribution is shown in Fig. 1. The sharp peak

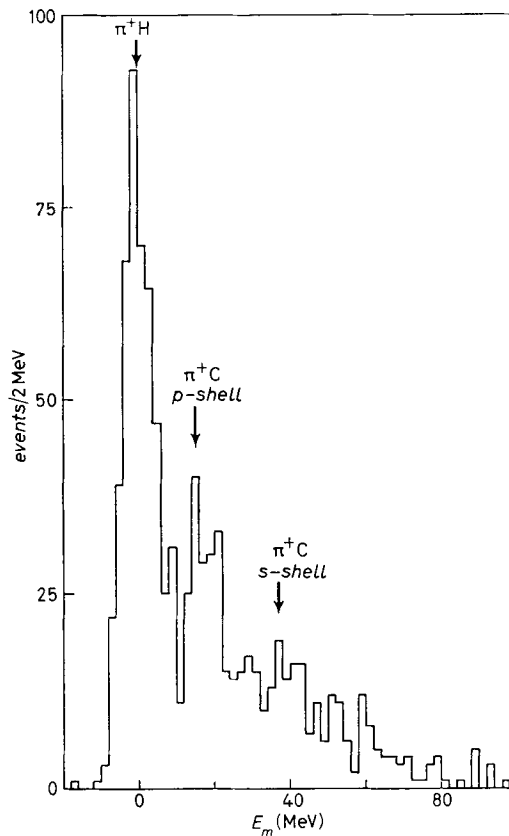


Fig. 1. - Missing energy ($E_m = T_{\pi_{\text{inc}}} - T_{\pi_{\text{out}}} - T_p$) distribution. The approximate E_m values for the elastic scattering on H, for the separation of a p -shell proton and s -shell protons are indicated.

around zero is due to elastic scatterings on H. Its position makes us sure of the beam energy evaluation and its width (~ 5 MeV of HWHM) gives a good estimate of the total energy resolution, which is limited by the energy spread of the beam and by the errors in the measurement of secondary particles.

The fit of each event has been tried for the following hypothesis:

$$\alpha) \pi^+ + p \rightarrow \pi^+ + p \text{ (4-constraints fit),}$$

and

$$\beta) \pi^+ + {}^{12}\text{C} \rightarrow \pi^+ + p + {}^{11}\text{B} \text{ (1-C fit).}$$

Events fitting α) and not β) are considered reactions on H; events fitting α) and β) are categorized according to their χ^2 probability and to their *a priori* probability, roughly evaluated from the ratio of events fitting α) or β) only. Events not fitting α) or β) have generally a high value of E_m and can be due to the reactions

$$(4) \quad \pi^+ + \text{C} \rightarrow \pi^+ + p + \text{B}^* \quad (E_m \simeq 35 \text{ MeV}),$$

where one s protons is emitted, or

$$(5) \quad \pi^+ + \text{C} \rightarrow \pi^+ + p + \dots \quad (E_m > 30 \text{ MeV}),$$

where more than one nucleon is emitted, but only one proton leaves a visible track.

A background of H interactions is still present in the sample of events classified as C reactions; in these background events the outgoing π makes a secondary inelastic interaction with emission of a very slow n or p and without an appreciable change in ionization; in these cases the apparent missing energy is different from zero but p_r is low. If we cut all events with a $p_r < 80$ MeV/c, this background is strongly suppressed.

The events that do not fit α) or β) are candidates for reaction (4). In order to eliminate the background due to reaction (5), we considered only events with a separation energy E_s , given by

$$E_s = E_m - p_r^2 / (2 \cdot m_B)$$

in the (26 ÷ 46) MeV interval. A further cut-off has been applied on the kinetic energy of the protons: events with $T_p < 20$ MeV have been rejected to lower the background of two-nucleon reactions.

The final samples consist of

153 events attributed to the separation of a proton from the p -shell,

95 events attributed to the separation of a proton from the s -shell.

1'4. *Charge exchange reactions.* — Charge exchange interactions can take place only on C nuclei. A γ -ray coming from the π^0 decay has a probability of 15 % to get (e^+ , e^-) pair or a Compton electron in the chamber fiducial volume. Then ~ 30 % of the charge exchange events are marked by at least a γ -ray. Due to the large radiation length of propane, compared with the bubble chamber dimensions, only few examples of two- γ events have been recorded and a full kinematical analysis is not possible. However, other confusing processes being absent, a pure although statistically poor sample of charge exchange events has been obtained.

1'5. *π^+ -neutron final state.* — There are 120 clean events candidates for the reaction (3). The background of in-flight decays, elastic or inelastic scatterings on C or on H with low momentum transfer to the proton, is easily eliminated by kinematical analysis. The remaining 108 events are mainly due to reactions on bound n, but contain a background from other nuclear events that will be considered later.

2. — Theory.

2'1. *The impulse approximation model.* — It has been suggested⁽³⁾ that the « quasi-free » scattering on bound nucleons can be interpreted by the impulse approximation model. For the particular reaction (1), that means the dominance of the Feynman diagram of Fig. 2. The corresponding matrix element can be

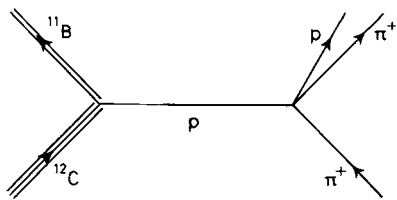


Fig. 2. — Feynman diagram for the reaction $\pi^+ + {}^{12}\text{C} \rightarrow \pi^+ + p + {}^{11}\text{B}$.

written as the product of the matrix element for the virtual decay ${}^{12}\text{C} \rightarrow p + {}^{11}\text{B}$, the matrix element for the π^+ -p scattering and the proton propagator. Let us introduce the following notations:

- p_j , E_j momentum and total energy of the particle j ;
- j , j' incoming and outgoing particle in the laboratory system;
- j^* , j'^* incoming and outgoing particle in the c.m. of the final π and p ;

⁽³⁾ I. S. SHAPIRO: *Rendiconti S.I.F.*, Course XXXVII (New York, 1967), p. 210.

- $E_{\bar{p}}$ total energy of the virtual proton;
 p_r momentum of the recoiling nucleus in the laboratory system;
 $\kappa = 2\sqrt{m_{Bp}\varepsilon}$, where m_{Bp} is the reduced mass of the system B-p and ε is the binding energy of the proton in ^{12}C (~ 16 MeV);
 γ^2 probability of a proton emission from the C nucleus;
 $|f(p_r)|^2$ form factor characterizing the momentum distribution of the virtual protons;
 $(d\sigma/d\Omega)^*$ cross-section for π -p in their centre of mass.

In the preceding notations, the differential cross-section can be written

$$(6) \quad \frac{d\sigma}{d^3p_B d^3p_{p'} d^3p_{\pi'}} = k\gamma^2 |f(p_r)|^2 \frac{(E_{\pi^*} + E_{p'}^*)^2}{(p_r^2 + \kappa^2)^2} \frac{(p_{\pi^*}/p_{\pi^*}^*)^2}{E_{\pi'} E_{p'} E_{\bar{p}}} (d\sigma/d\Omega)^* \cdot \delta(\mathbf{p}_C + \mathbf{p}_{\pi} - \mathbf{p}_B - \mathbf{p}_{\pi'} - \mathbf{p}_{p'}) \delta(E_C + E_{\pi} - E_{\pi'} - E_{p'} - E_B),$$

where k is a numerical constant.

In order to compute explicitly the cross-section some simplifications have been made:

$$E_{\bar{p}} = M_p \quad \text{and} \quad p_{\pi^*}/p_{\pi^*}^* = 1;$$

the two preceding simplifications are in agreement with the spirit of the model, *i.e.* the scattering $\pi(p) \rightarrow \pi p$ is quasi-free and the virtual proton is not relativistic.

Some problems arise with the π -p cross-section. The initial proton being virtual, $d\sigma/d\Omega$ that appears in formula (6) depends on s , the total energy of the π -p in their c.m., on t , the momentum transfer from the incoming to the outgoing pion, and on μ^2 , mass of the virtual proton. The first approximation consists in putting $d\sigma(s, t, \mu^2)/d\Omega = d\sigma(s, t, m_p^2)/d\Omega$. Moreover the physical region for (s, t) in the scattering on bound nucleons is different from that for free scattering as is shown in Fig. 3. If, for a given s , the calculated t is out of the allowed range for the free scattering at the same s , we calculated $d\sigma/d\Omega$ on the boundary of the physical region at the same s . The results of the calculations change slightly if the value of $d\sigma/d\Omega$ is taken on the physical boundary at the same t ; then we are confident in our procedure. The values used for the total and differential cross-sections are the experimental ones ⁽⁴⁾.

In the first stage of the computation the form factor has been taken constant and it will be calculated from the experimental data (Subsect. 3'1).

(4) V. S. BARASHENKOV and V. M. MALTSEV: *Cross-Sections of Elementary Particle Interactions* (Moscow, 1966).

The most important predictions of the model have been discussed in ⁽³⁾. Those that can be checked in the present experiment are

the Treiman-Yang (T.Y.) angle Φ defined by

$$\cos \Phi = \frac{(\mathbf{p}_C \times \mathbf{p}_B) \cdot (\mathbf{p}_\pi \times \mathbf{p}_D)}{|\mathbf{p}_C \times \mathbf{p}_B| |\mathbf{p}_\pi \times \mathbf{p}_D|},$$

where all the momenta are in the system of the incident π , is uniformly distributed;

the momentum distribution of the recoiling nucleus is limited to low values, due to the presence of the propagator and of the form factor;

ratios between cross-sections for interactions on a p or on a n must be the same as for free reactions, apart from a kinematical factor.

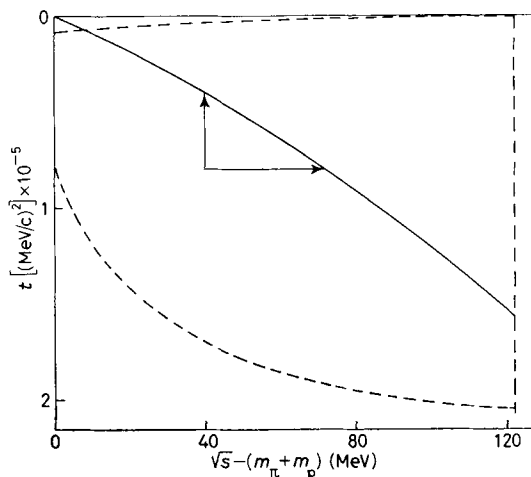


Fig. 3. - (\sqrt{s}, t) -plane. The physical region for scattering on free protons is bounded by the \sqrt{s} -axis and by the continuous line; the physical region for the scattering on bound protons, calculated for an energy of the incoming π of about 130 MeV, is delimited by the dashed lines.

To obtain quantitative predictions from formula (6), the knowledge of γ^2 and of the form factor is needed. The model does not contain in itself any prescription for γ^2 and $f(p_r)$; they must be measured or calculated from other theoretical models.

2.2. Experimental distortions. - The theoretical predictions cannot be directly compared with the experimental data, which are biased by the method of selecting the events. The experimental distortions have been evaluated by a calculations based on Monte Carlo method. Let x be the set of variables de-

fining completely the configuration of an event and ξ the set of variables defining its position and orientation in the bubble chamber frame. An event is completely defined in our experimental apparatus by x and ξ ; let us indicate it by $E(x, \xi)$. About 10 000 pseudoevents have been generated for each channel according to the phase-space probability, using as starting point 2000 primary π 's and interaction points previously measured.

Some kinematical regions turned out poorly populated: more other pseudoevents have been generated to obtain a significant statistics in each bin.

Charged tracks have been followed up to the point where they interact or stop or leave the chamber. The π 's have been allowed to decay into two γ 's and, for each γ , it has been calculated the probability of manifesting itself in an electron-positron pair or in a Compton electron, taking into account the energy dependence of the two processes.

At this stage it was easy to apply to the pseudoevents the same cut-off imposed to the real ones; then we got two samples of pseudoevents: visible events, indicated by $E^{\text{vis}}(x, \xi)$, *i.e.* events that, if real, would be retained, and invisible events.

A weight $T(x)$, equal to the theoretical density of probability (the phase-space factor excluded), was given to each event and two sets of weights were obtained:

$T^{\text{vis}}(x, \xi)$ weights of visible events $E^{\text{vis}}(x, \xi)$,

$T(x, \xi)$ weights of all the events.

The fraction V of visible events is given by the ratio

$$(7) \quad V = \frac{\sum_{x, \xi} T^{\text{vis}}(x, \xi)}{\sum_{x, \xi} T(x, \xi)}.$$

In the IAM hypothesis and with the form factor calculated in Subsects. 3'1 and 3'2 the values of V are

Final state	π^+p		π^+n		π^0p	
shell	p	s	p	s	p	s
V	0.40	0.49	0.43	0.63	0.31	0.31

The corrected differential distributions are the weighted distributions of visible events $E^{\text{vis}}(x, \xi)$.

3. - Analysis of the data.

3'1. *Reactions on protons of the p-shell.* - The first check on the validity of the IAM is given by the shape of the T.Y. angular distribution. In principle

it does not depend on the form factor and must be flat; because of the experimental biases, also this distribution depends on the form factor, but very weakly.

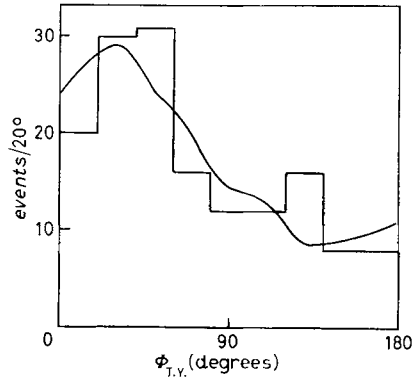


Fig. 4. — Treiman-Yang-angle distribution for p -shell protons.

In Fig. 4 data and theoretical prediction are compared; the agreement is reasonably good ($\chi^2 = 8/8$ n.d. corresponding to a 35 % confidence level). To compare other distributions we need the explicit shape of the form factor.

Determination of the form factor. It has been suggested ⁽³⁾ that the form factor (f.f.) of the nuclear vertex does not depend on the particular reaction occurring at the second vertex. As a consequence the f.f. for the present reaction must be the same as for stripping reactions at low energy; this indicates a f.f. of the shape

$$(8) \quad f(p_r) = \sin(R \cdot p_r) + \frac{(\kappa R)^2}{1 + \kappa R} \left[\frac{\sin(R \cdot p_r)}{(R \cdot p_r)^2} - \frac{\cos(R \cdot p_r)}{R \cdot p_r} \right],$$

where R is practically equal to the C radius and κ has been defined in 2'1. This f.f. has zeros at $p_r = 0, \sim 175, \sim 300 \dots$ MeV/c and it is clearly incompatible with our experimental distribution of p_r (Fig. 5). Then we have assumed a f.f. of exponential shape

$$(9) \quad |f(p_r)|^2 \propto p_r^2 \exp[-(p_r/A_p)^2].$$

The parameter obtained for the p -state from the simple harmonic-oscillator functions A must be fitted on the data.

The three form factors shown in Fig. 6 are

- 1) Butler form factor given by expression (8),
- 2) the harmonic-oscillator form factor for p -proton (9), and
- 3) the same for s -proton (10) given in Subsect. 3'2.

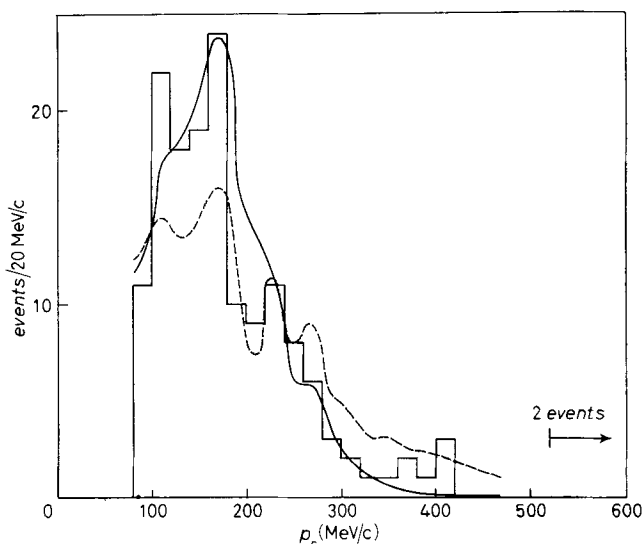


Fig. 5. — Recoil momentum distribution. The dashed line corresponds to the prevision with a constant form factor ($|f(p_r)|^2 \propto \text{const}$); the continuous line corresponds to the factor $|f(p_r)|^2 \propto p_r^2 \exp[-(p_r/A)^2]$, where $A = 160$ MeV/c.

The best estimation of A_p for $p_r > 80$ MeV/c is (160 ± 10) MeV/c; the corresponding χ^2 is 14/11 n.d.; the experimental resolution on p_r (~ 10 MeV/c) has been taken into account. The χ^2 for the constant form factor is 20/12 n.d.: a form factor of the type (9) is preferred (Fig. 5).

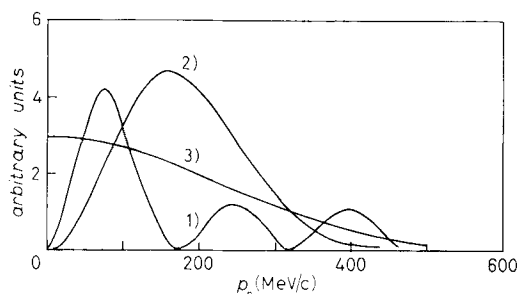


Fig. 6. — Form factors corresponding to 1) formula (8) of the text, 2) harmonic oscillator for p -shell protons and 3) harmonic oscillator for s -shell protons.

Angular and invariant-mass distributions. The form factor having been determined, we can check other predictions of the model. In Fig. 7 the angular distributions of the outgoing particles in the c.m. system are shown.

The experimental resolution has not been folded in the theoretical curve because its effect is negligible. The agreement with the theoretical predictions is generally satisfactory. These distributions are very weakly affected by the form factor and, with the exception of the outgoing π , also the visibility does

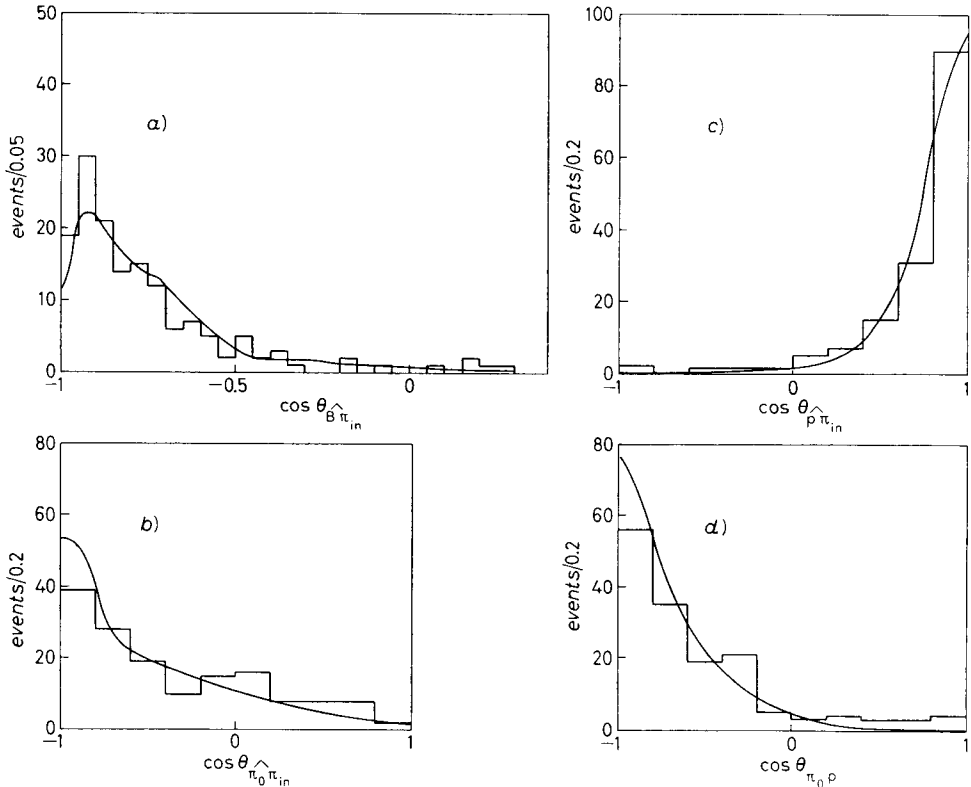


Fig. 7. - Angular distributions between a) ^{11}B and incoming π^+ , b) incoming and outgoing π^+ , c) proton and incoming π^+ , d) proton and outgoing π^+ . All variables are in the c.m. system. The continuous line (here and in the following Figures) is the prediction of formula (6) with the exponential form factor.

not introduce important distortions; then the comparison with the predictions is reliable.

In Fig. 8 the three invariant-mass distributions are shown. The agreement in the π -p Q value is rather poor, the theoretical curve seeming shifted towards the high values. The two other distributions, although strongly distorted by the visibility, agree remarkably with the calculations.

We conclude that, within the present statistics and measurement accuracy, there are no large deviations from the theoretical predictions.

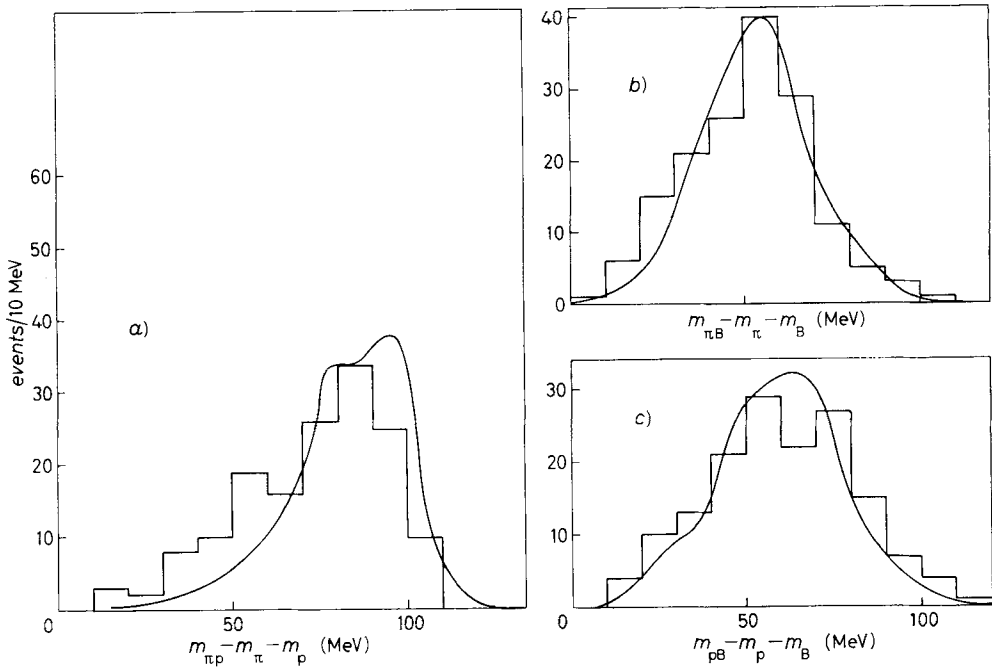


Fig. 8. — Invariant-mass distributions for a) π -p, b) π - ^{11}B and c) p - ^{11}B .

3'2. Reactions on protons of the s -shell. — The predictions of formula (6) have been calculated also for interactions on protons of the s -shell. In this case the separation energy is not sharply defined; the central value, measured in $(p, 2p)$ experiments ⁽⁵⁾, is 34 MeV and the half-width ~ 9 MeV. The IAM

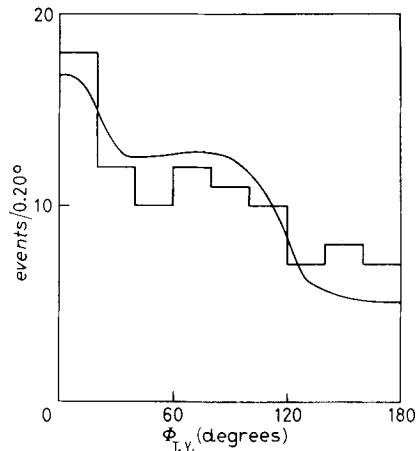


Fig. 9. — Treiman-Yang-angle distribution for s -shell protons.

⁽⁵⁾ H. TYREN, S. KULLANDER, O. SUNDBERG, R. RAMACHANDRAN and P. ISACSSON: *Nucl. Phys.*, **79**, 321 (1966).

calculation has been carried out using a fixed value of 35 MeV and then the predictions are less precise than for p -protons.

Figure 9 shows the distribution of the T.Y. angle, which agrees with the theoretical predictions. The form factor for s -protons, obtained from the harmonic-oscillator functions as for p -protons, has the shape

$$(10) \quad |f(p_r)|^2 \propto \exp [-(p_r/A_s)^2].$$

The best value of A_s is

$$A_s = (300 \pm 30) \text{ MeV/c},$$

the corresponding χ^2 is 14.8/7, while the χ^2 for constant f.f. is 30/8 n.d. In Fig. 10 the p_r distribution is reported together with the theoretical predictions.

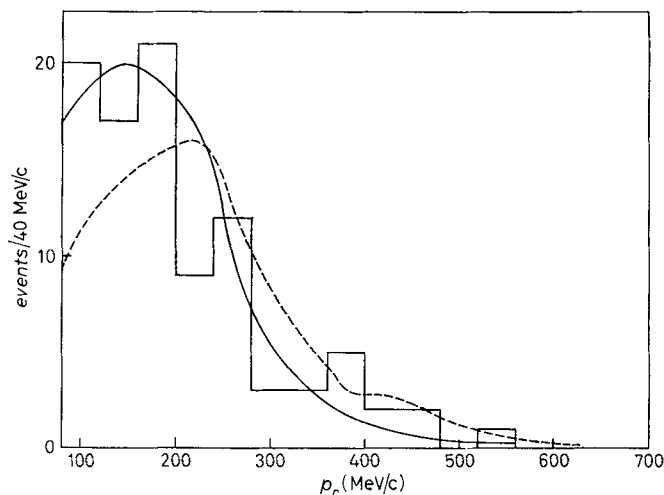


Fig. 10. — Recoil momentum distribution. The dashed line is calculated with constant form factor ($|f(p_r)|^2 \propto \text{const}$); the continuous line with an exponential form factor $|f(p_r)|^2 \propto \exp [-(p_r/A)^2]$, where $A = 300 \text{ MeV/c}$.

Angular distributions are shown in Fig. 11. Fig. 12 shows the invariant-mass distributions; they are in qualitative agreement with the IAM predictions. The agreement could be improved if we take into account the separation energy spread, the effect of which would result in a smearing of the invariant masses. The agreement between theory and experimental data is good enough to conclude that the model accounts also for the quasi-« free scattering » on strongly bound protons as the protons of the s -shell are.

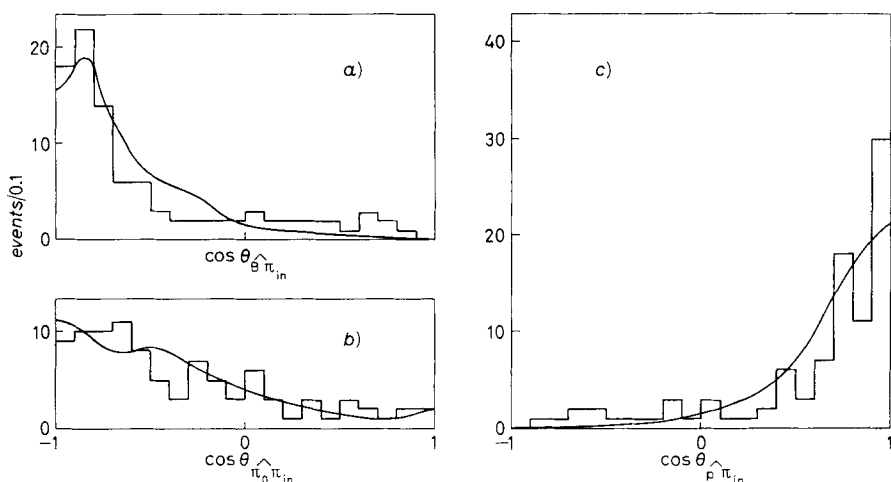


Fig. 11. — Angular distribution between a) ^{11}B and incoming π^+ , b) outgoing and incoming π^+ and c) p and incoming π^+ . All distributions are in the c.m. system.

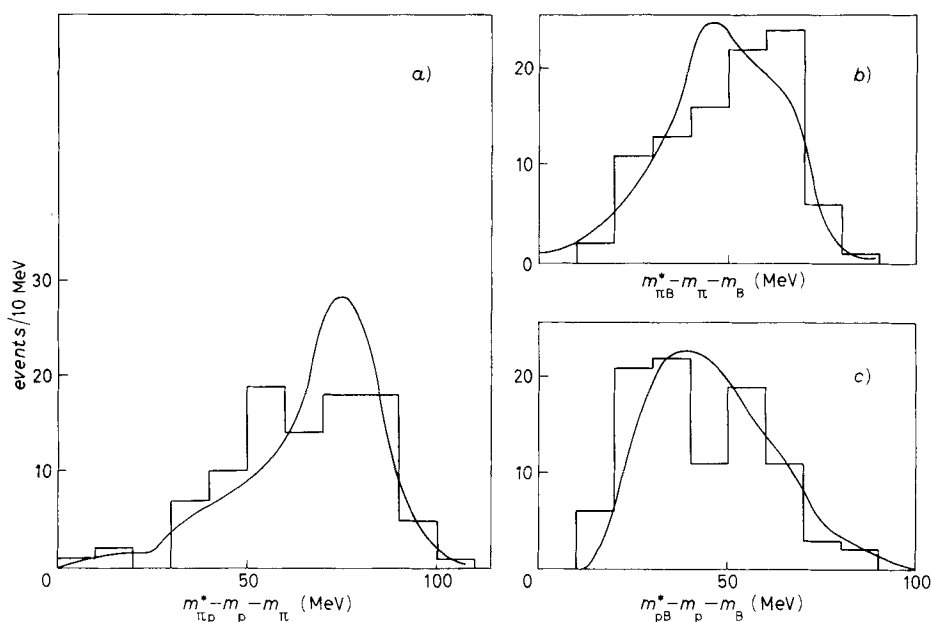


Fig. 12. — Invariant-mass distributions for a) π -p, b) π - ^{11}B and c) p- ^{11}B .

3.3. Probability of extraction of a p- and an s-proton. — It is now possible to evaluate the ratio between the cross-sections σ_p and σ_s for the separation of a proton from the shells p and s. The number of events, corrected for background mainly due to reactions followed by two nucleons emission and for

losses due to bad measured events, is 150 and 123 respectively. Taking into account the visibility factors (see 2'2), the final numbers are 375 events on p -protons and 251 events on s -protons. The ratio is

$$(11) \quad R_{p/s} = \sigma_p/\sigma_s = 1.5 \pm 0.2;$$

the error is the statistical one.

3'4. Charge exchange reactions. — As pointed out in 1'4, a complete kinematical analysis of the charge exchange events is not possible and then it is difficult to separate different nuclear reactions. In order to minimize the background of many-nucleon emissions, the events with a low-energy proton ($T_p < 20$ MeV) have been eliminated; 54 events are left for the analysis. The IAM predictions have been calculated assuming a f.f. and a ratio σ_p/σ_s for neutrons equal to those obtained for protons; also the charge exchange differential cross-section has been assumed equal to the $\pi^+p \rightarrow \pi^+p$ cross-section. The angular and energy distributions of the visible γ -ray and of the proton are shown in Fig. 13 and 14, together with the theoretical predictions.

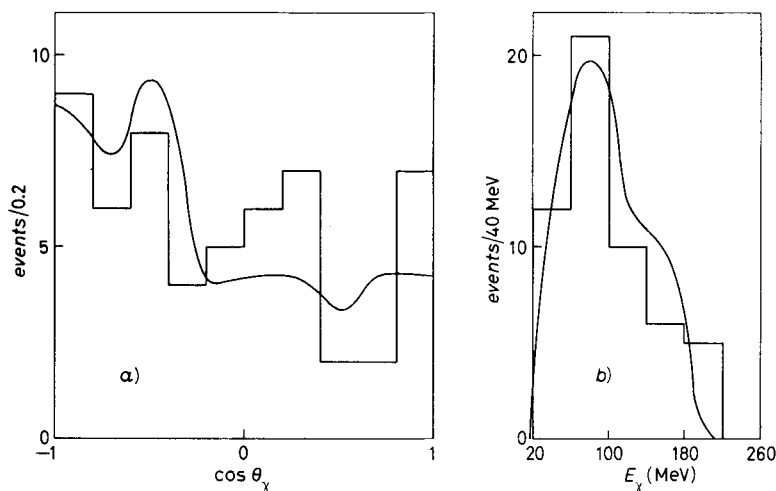


Fig. 13. — Charge exchange events in the laboratory system: *a*) angular distribution and *b*) energy distribution of γ -rays.

The agreement, in the limit of the few kinematical variables at our disposal and of the statistics, is good.

The number of charge exchange events, corrected for γ loss and for the cut-off on T_p , is 174. The ratio between the cross-sections for separation of a proton and for charge exchange is

$$(12) \quad R_{\pi^+p/\pi^+p} = \frac{\sigma_{\pi^+(p) \rightarrow \pi^+p}}{\sigma_{\pi^+(n) \rightarrow \pi^+p}} = 3.6 \pm 0.6.$$

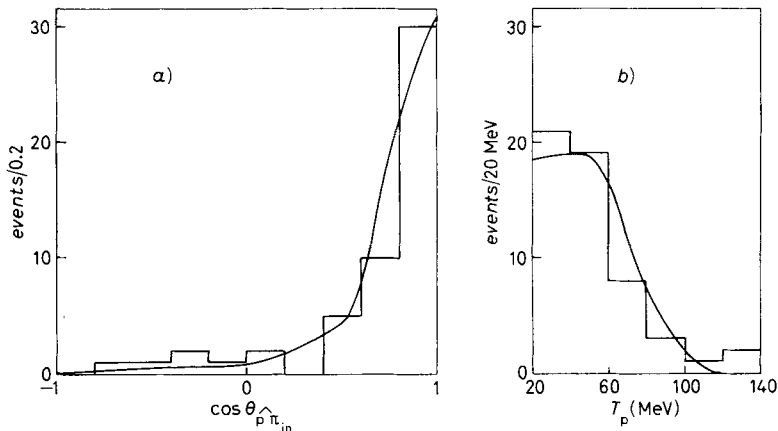


Fig. 14. - Charge exchange events in the laboratory system: *a*) angular distribution and *b*) kinetic-energy distribution of outgoing protons.

3.5. π^+ -neutral events. - The events showing only a π^+ in the final state can be ascribed to various nuclear reactions:

- i) $\pi^+ + C \rightarrow \pi^+ + C^*$, where the C is left in a high excited state;
- ii) $\pi^+ + C \rightarrow \pi^+ + mN + X$, where more than one nucleon is extracted and the protons leave a nondetectable track;
- iii) $\pi^+ C \rightarrow \pi^+ + n + {}^{11}C$, where a n from the *p*- or *s*-shell is separated.

The contribution from i) is small (≤ 4 events) and has been evaluated by using the data of BINON *et al.* ⁽⁶⁾. Background from ii) (~ 14 events) has been estimated by assuming a fraction of two-neutron events equal to the ratio of $\pi^+ 2p$ over $\pi^+ p$ events.

The comparison of our data and the IAM predictions, calculated as for charge exchange reactions, is not completely reliable owing to the presence of a total background of 20 %. In any case data and calculated predictions for angle and energy of the outgoing π^+ and for the missing momentum are shown in Fig. 15. While distributions *a*) and *c*) of this Figure do not show important deviations from the predictions, the π^+ energy is in disagreement with the calculations. The background of 2n emission gives a contribution in the low-energy region of the spectrum and the disagreement is stronger than in the Figure.

Under the assumption that our calculation is sufficiently accurate to give a correct visibility factor, the corrected number of events is 176. The

⁽⁶⁾ F. BINON, P. DUTEIL, J. P. GARRON, J. FORRES, L. HUGON, J. P. PEIGNEUX, C. SCHMIT, M. SPIGHEL and J. P. STROOT: *Nucl. Phys.*, **17 B**, 168 (1970).

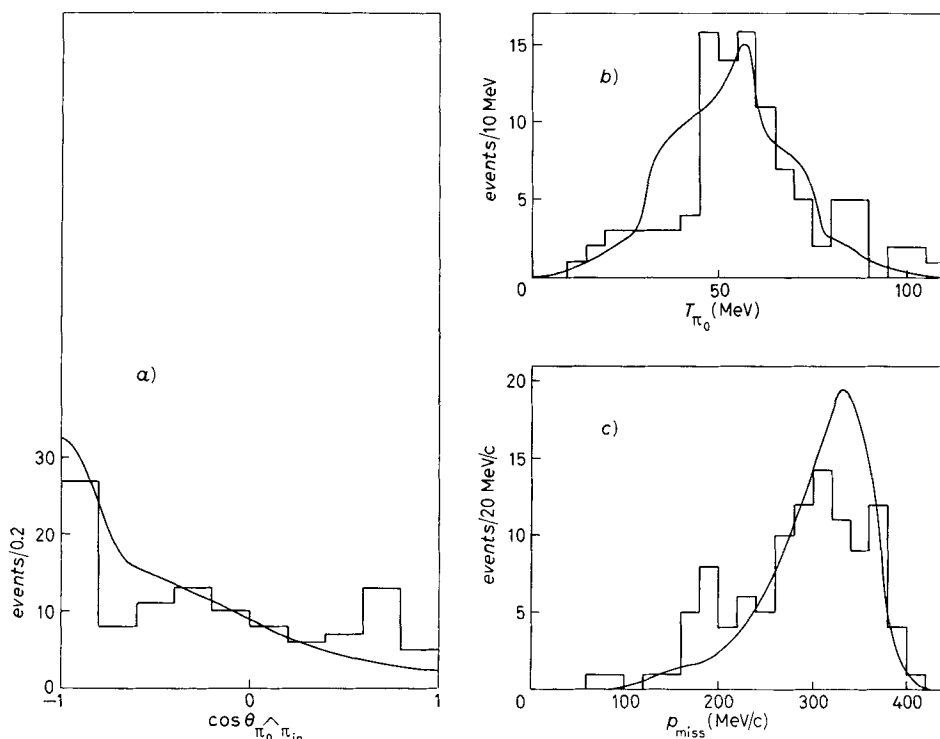


Fig. 15. - π^+ -neutral events: *a*) angular distribution and *b*) kinetic-energy distribution for the outgoing π^+ , *c*) missing-momentum distribution.

ratios of the cross-sections for reaction iii) are

$$(13) \quad R_{\pi^+p/\pi^+n} = \frac{\sigma_{\pi^+(p) \rightarrow \pi^+p}}{\sigma_{\pi^+(n) \rightarrow \pi^+n}} = 3.5 \pm 0.4$$

and

$$(14) \quad R_{\pi^+n/\pi^0p} = \frac{\sigma_{\pi^+(n) \rightarrow \pi^+n}}{\sigma_{\pi^+(n) \rightarrow \pi^0p}} = 1.0 \pm 0.2.$$

3'6. Cross-sections. The absolute cross-section for the (π^+, π^+p) reactions has been estimated by comparing the number of events in the (π^+, π^+p) channel with the number of elastic events on H measured on $\sim \frac{2}{3}$ of the pictures used. In the energy interval $(115 \div 150)$ MeV we obtain

$$\sigma_{(\pi^+, \pi^+p)} = (66 \pm 10) \text{ mb}$$

(error takes into account also various corrective factors).

From the (π^+ , π^+p) cross-section, all other cross-sections have been obtained; they are reported in Table I.

TABLE I.

Final state	π^+p	π^+p	π^0p	π^+n	$\pi^0 \dots$
	<i>p</i> -shell	<i>s</i> -shell	(<i>p</i> + <i>s</i>)-shells	(<i>p</i> + <i>s</i>)-shells	total charge exchange
Cross-section (mb)	40 ± 5	26 ± 9	18 ± 3	18 ± 3	36 ± 5

4. - Discussion.

4.1. *Differential cross-sections and form factor.* - From the comparison of our data with the theoretical predictions, we can conclude that:

a) The model accounts for a large fraction of the $\pi^+(p) \rightarrow \pi^+p$ events; that seems to be true both for *p*- and *s*-shell protons.

b) The harmonic-oscillator form factors (9) and (10) are preferred to a Butler f.f. or to a constant f.f. The best estimates for the parameters A_p and A_s are $A_p = (160 \pm 10)$ MeV/c and $A_s = (300 \pm 30)$ MeV/c.

c) Although the agreement between data and calculations is generally good, some deviations from the predictions appear in the invariant π^+p mass distribution (Fig. 8 and 12).

d) No deviations from the predictions are observable in the π^+B or pB invariant masses.

These results are in substantial agreement with those of two other similar experiments. GISMATULLIN and OSTROUMOV⁽⁷⁾ have studied the quasi-free scattering on bound proton in light nuclei by mean of nuclear emulsions at 117 MeV. They do not carry out a complete comparison with any model. They find a flat distribution for the T.Y. angle for $p_r < 200$ MeV/c, while, for $p_r > 200$ MeV/c, the agreement of their data with the flat distribution is not so good. The p_r distribution has a maximum around 100 MeV/c and does not exhibit the sharp minimum required by a f.f. of the type (8), but it has a smooth fall-off as qualitatively expected if the f.f. is exponential.

The $\pi^-(p) \rightarrow \pi^-p$ on C has been investigated by AGANYANTS *et al.*⁽⁸⁾ at 1.04 GeV/c, in the region of the Δ_3 -resonance. They compare their data with

(7) V. I. OSTROUMOV and YU. R. GISMATULLIN: *Sov. Journ. Nucl. Phys.*, **11**, 159 (1970).

(8) A. O. AGANYANTS, YU. D. BAYNKOV, V. N. DEZA, S. V. PONSKOV, V. B. FEDOROV, N. A. IVANOVCI, V. D. KHOVANSKY, V. M. KOLYBASOV, G. A. LESKIN, V. L. STOLIN and L. S. VOROBYER: *Nucl. Phys.*, **11** B, 79 (1969).

the Feynman graph of Fig. 2 and find a general agreement for $p_r < 135$ MeV/c. The p_r distribution is compared only with a f.f. of the type (8); theory and data have completely different trends for $p_r > 135$ MeV/c.

There are no experiments on π -C interactions in which the exponential f.f.'s are tested; so we compare our result with (p, 2p) and (e, e'p) data.

RIOU⁽⁹⁾ finds, from (p, 2p) data at 155 and 460 MeV,

$$A_p = 75 \quad \text{and} \quad A_s = 150.$$

SIMPSON *et al.*⁽¹⁰⁾ at 1 GeV:

$$A_p = 130 \quad \text{and} \quad A_s = 135.$$

AMALDI *et al.*⁽¹¹⁾, in (e, e'p) reactions at ~ 600 MeV, obtain

$$A_p = 94 \pm 8 \quad \text{and} \quad A_s = 157 \pm 18.$$

The discrepancy with our results is apparent; in fact these authors analysed their data using the PWIA or DWIA, while we compared our data with the graph of Fig. 2.

In our case the proton propagator acts as damping and the width of the f.f.'s results greater. If the propagator is not considered in formula (6), we obtain

$$A_p \simeq 120 \quad \text{and} \quad A_s \simeq 150 \text{ MeV/c} \quad \text{respectively.}$$

In spite of some discrepancies between model and data, it seems reasonable to conclude that the model gives a satisfactory general description of the angular and energetic distributions.

It must be noted that data are not completely free from backgrounds of various kinds. For instance, it is known from a (p, 2p) experiment⁽¹²⁾ that cross-sections for reactions leading to ^{11}B in a low excited states (2.14, 4.46, 5.04, 6.76 MeV) are not completely negligible, while we assumed that the B is always left in the ground state. Moreover in the s -shell proton events, a background of two-nucleon emission certainly exists, the separation energy for two nucleons being of the same magnitude as the energy needed for the extraction

⁽⁹⁾ M. RIOU: *Rev. Mod. Phys.*, **37**, 375 (1965).

⁽¹⁰⁾ W. D. SIMPSON, J. L. FRIEDES, H. PALEVSKI, R. J. SUTTER, G. W. BENNET, B. GOTTSCHALK, G. IGO, R. L. STEARNS, N. S. WALL, D. M. CORLEY and G. C. PHILLIPS: *Nucl. Phys.*, **140** A, 201 (1970).

⁽¹¹⁾ U. AMALDI jr., G. CAMPOS VENUTI, G. CORTELESSA, C. FRONTEROTTA, A. REALE and P. SALVADORI: *Phys. Rev. Lett.*, **13**, 341 (1964); *Phys. Lett.*, **25** B, 24 (1967).

⁽¹²⁾ T. YUASA and E. HOURANY: *Nucl. Phys.*, **103** A, 577 (1967).

of an s proton. A greater total energy resolution (≤ 1 MeV) must be achieved to really test the model.

Regarding the charge exchange process, we can simply conclude that our results are in agreement with the predictions; up to now no experiment that gives a complete reconstruction of the reaction kinematics exists (at least to our knowledge).

Finally we observe that our data on the $\pi^+(n) \rightarrow \pi^+n$ reaction are in bad agreement with the model; unfortunately our experimental technique is inappropriate to study such a process, then we cannot arrive at any firm conclusion on this point, but we can take our result as a suggestion that deviations from the simple IAM here used could be more detectable in the π^+n channel.

4'2. σ_p/σ_s ratio. — No other experiment gives the ratio σ_p/σ_s for π at our energy. YUASA and HOURANY⁽¹²⁾ give a lower limit for the $(p, 2p)$ reaction; they find

$$\sigma_{(p, 2p)_p}/\sigma_{(p, 2p)_s} < 3$$

at 100 MeV; SIMPSON *et al.*⁽¹⁰⁾ collect 83 and 104 events respectively on p and s protons at 1 GeV, but they do not give the ratio corrected for their geometry. These values are very similar to our result (11), but the comparison is not really meaningful because of the different values of the primary energy and the different energy dependence of the free cross-sections.

4'3. Ratios among $\sigma_{(\pi^+, \pi^+p)}$, $\sigma_{(\pi^+, \pi^0p)}$ and $\sigma_{(\pi^+, \pi^+n)}$. — The ratios among the three channels (π^+, π^+p) , (π^+, π^0p) and (π^+, π^+n) can be computed by means of formula (6). Using the experimental cross-sections ($\sigma_{\pi^+n} = \sigma_{\pi^-p}$) for the three processes, the following figures have been obtained:

$$R_{\pi^+p/\pi^0p} = 3 \quad \text{and} \quad R_{\pi^+p/\pi^+n} = 8.$$

These values differ from 4.5 and 9, as they are predicted by the $I = \frac{3}{2}$ dominance, because the values of the free cross-section do not respect in all the interested energy range the values predicted by the $I = \frac{3}{2}$ dominance. The same argument has been used by KOLYBASOV⁽¹³⁾ to compute the ratio $R_{\pi^-n/(\pi^+n+\pi^0p)}$ and he obtained 1.5 ± 0.15 not in contrast with our result, in the assumption $\sigma_{\pi^+p} = \sigma_{\pi^-n}$.

Our experimental result (12) on the charge exchange channel is in good agreement with the prediction, while the experimental ratio (13) is much lower than the predicted one.

(13) V. M. KOLYBASOV: *Journ. Nucl. Phys.*, **2**, 101 (1966); *Phys. Lett.*, **27** B, 3 (1968).

Our result can be compared, under the assumption that $\sigma_{\pi^+\text{p}} = \sigma_{\pi^-\text{n}}$, with the ratio

$$(15) \quad R_{\pi^-\text{n}/(\pi^+\text{n}+\pi^0\text{p})} = 1 \pm 0.1$$

measured in ⁽¹⁾ by the radiochemical method at 180 MeV. We obtain

$$R_{\pi^+\text{p}/(\pi^+\text{n}+\pi^0\text{p})} = 1.7 \pm 0.2.$$

In order to explain the disagreement of Fig. 15 with the value of 3, expected on the basis of a crude application of the $I = \frac{3}{2}$ dominance, many theoretical suggestions have been proposed.

We will consider first the calculation of ROBSON ⁽¹⁴⁾, who takes into account the interaction between the final nucleon \mathcal{N} and the residual nucleus X . The isotopic spin of \mathcal{N} and X can be 0 or 1, then the three cross-sections can be written, if we assume a pure $I = \frac{3}{2}$ state for the $\pi\text{-}\mathcal{N}$ couple,

$$\begin{aligned} \sigma_{\pi^+\text{p}} &\propto |A_1 + 2A_0|^2, \\ \sigma_{\pi^+\text{n}} &\propto |-A_1 + 2A_0|^2, \\ \sigma_{\pi^0\text{p}} &\propto |\sqrt{2}A_1|^2, \end{aligned}$$

where A_1 and A_0 are assumed equal. In case of no final-state interaction, the two amplitudes interfere completely, while in the opposite case of formation of a compound nucleus, the two amplitudes do not interfere. In the case of partial interference, it is possible to write

$$\sigma_{\pi^+\text{p}} \propto 5 + 4\kappa, \quad \sigma_{\pi^+\text{n}} \propto 5 - 4\kappa \quad \text{and} \quad \sigma_{\pi^0\text{p}} \propto \sqrt{2},$$

where κ , that is an indicator of the degree of final-state interaction, ranges from 1 to 0. The first prediction of this model is that the ratio $\pi^0\text{p}/(\pi^+\text{p}+\pi^+\text{n})$ always assumes the predicted value 4.5. The values of κ estimated from our data are

$$\kappa_{\pi^0\text{p}} = 0.55 \pm 0.30 \quad \text{and} \quad \kappa_{\pi^+\text{n}} = 0.69 \pm 0.06.$$

These figures are compatible between them but are much higher than the value $\kappa = 0.25$ evaluated using the data of CHIVERS *et al.* Such a strong variation of κ with the energy and the fact that at lower energy the final-state interaction seems less important are unclear. This argument is true also if contributions from an $I = \frac{1}{2}$ state are considered, the point being that our results are nearer to the predicted values than those of CHIVERS.

⁽¹⁴⁾ D. ROBSON: *Final-state interactions and the charge dependence of $(\pi, \pi\mathcal{N})$ reactions from nuclei*, preprint.

SEKI⁽¹⁵⁾ considers all the possible cases for the isotopic structure of the π -C reactions. He takes into account the values of $\frac{1}{2}$, $\frac{3}{2}$ and $\frac{5}{2}$ for the I -spin of the residual nucleus and calculates the ratios under the hypothesis that a particular two-particle isospin state is enhanced. Among the three possible solutions, an enhancement in the $I = 0$ N -X state prohibits the charge exchange reaction. If our charge exchange events are due to only one proton emission, that hypothesis must be discarded; moreover any strong enhancement in the p -B invariant mass is detected. The hypothesis of a mixture of I -states of the residual nucleus cannot be ruled out because, in the present experiments, the final state of the residual nucleus is not completely identified.

* * *

We should like to thank Dr. M. ROLLIER, who participated to the early stage of this experiment, and A. PULLIA for many enlightening discussions.

We are indebted to Prof. E. FIORINI for his continuous support, encouragement and advice; we thank him for his kind criticism of the manuscript too.

Thanks are due to the programming and scanning teams of our laboratory, especially to Mr. U. BEGGI for his help in the data collection.

It is a pleasure to thank the Ecole Polytechnique, Orsay and Saclay groups, who carried out the exposure in Saclay and made this experiment possible.

(15) R. SEKI: *The puzzle of $^{12}\text{C} \rightarrow ^{11}\text{C}$ reactions with pion near the pion-nucleon 3-3 resonance*, preprint.

● RIASSUNTO

Sono state studiate le reazioni (π^+ , πN) a ~ 130 MeV (energia cinetica) mediante una camera a bolle a propano. Sono stati analizzati circa 250 eventi di diffusione quasi elastica su protoni legati dei livelli p ed s ed i risultati ottenuti sono stati confrontati con le predizioni del modello dell'approssimazione degli impulsi (IAM): l'accordo è generalmente buono. Abbiamo ottenuto i seguenti risultati: i valori migliori per il parametro A che compare nei fattori di forma dell'oscillatore armonico sono $A_p = (160 \pm 10)$ MeV/c e $A_s = (300 \pm 30)$ MeV/c per i protoni del livello p ed s rispettivamente; la sezione d'urto totale per la reazione (π^+ , π^+p) è (66 ± 10) mb ed il rapporto tra le sezioni d'urto per la separazione di un protone p o di un protone s è 1.5 ± 0.2 . Sono stati selezionati circa 100 eventi di scambio carica; la sezione d'urto corrispondente è (36 ± 5) mb mentre la σ stimata per (π^+ , π^0p) è (18 ± 3) mb. Nel limite della statistica sembra che anche questa reazione possa essere spiegata sulla base del IAM. I dati riguardanti le reazioni (π^+ , π^+n) basati su ~ 100 eventi mostrano, con le predizioni del IAM, qualche discrepanza che non può facilmente essere spiegata per la bassa statistica e le difficoltà dell'analisi sperimentale. Il rapporto tra le sezioni d'urto per la separazione di un protone e di un neutrone è 1.7 ± 0.2 .

Реакции (π^+ , π^0) на углероде при 130 МэВ.**Эксперимент в пузырьковой камере.**

Резюме (*). — В пропановой пузырьковой камере были исследованы реакции (π^+ , π^0) при кинетической энергии ~ 130 МэВ. Было проанализировано около 250 событий квази-упругого рассеяния на связанных протонах p и s оболочек. Полученные результаты сравниваются с предсказаниями модели импульсного приближения и получается хорошее согласие. Мы получили следующие результаты: наилучшие значения для параметра A , появляющегося в форм-факторах гармонического осциллятора, составляют $A_p = (160 \pm 10)$ МэВ/с и $A_s = (300 \pm 30)$ МэВ/с соответственно для протонов p и s оболочек; полное поперечное сечение для реакции (π^+ , π^+p) равно (66 ± 10) мб и отношение между поперечными сечениями для отрыва p или s протона составляет 1.5 ± 0.2 . Были отобраны около 100 событий с перезарядкой. Соответствующее поперечное сечение составляет (36 ± 5) мб, тогда как вычисленное σ для реакции (π^+ , π^0p) равно (28 ± 3) мб. В пределе большой статистики, по-видимому, эта реакция также может быть объяснена на основе модели импульсного приближения. Данные, относящиеся к реакциям (π^+ , π^+n), основанные на анализе ~ 100 событий, обнаруживают некоторые расхождения с предсказаниями модели импульсного приближения, которые не могут быть объяснены малой статистикой и трудностями экспериментального анализа. Отношение между поперечными сечениями для отрыва p и n составляет 1.7 ± 0.2 .

(*) *Переведено редакцией.*